Asymmetric Effects in Forced VDE Modeling

C. R. Sovinec and K. J. Bunkers

University of Wisconsin-Madison

Center for Tokamak Transient Simulation

November 4, 2018 Portland, Oregon

Center for Tokamak Transient Simulation

Introduction

- Visco-resistive MHD NIMROD computations are being applied to understand asymmetric VDE physics.
  - Thermal quench
  - Current spike
  - Current quench
  - Wall forcing
- In analogy to experimental VDE studies, our computations for an idealized configuration consider forced vertical displacement.
  - On JET, VDE studies used programmed displacement [Riccardo, et al., PPCF **52**, 124018].

Parameters and closure relations define the MHD model.

- Magnetic diffusivity depends on temperature.
  - $\eta(T) = \min\left[\eta_0 \left(T_0/T\right)^{3/2}, 1\right]$
  - $S = \tau_\eta / \tau_A = \mu_0 a^2 / \eta_0 \tau_A \cong 1 \times 10^6$
- Thermal conduction and viscous stress are anisotropic with fixed coefficients.
  - $\mathbf{q} = -n\left[\left(\chi_\| - \chi_{iso}\right)\hat{\mathbf{b}}\hat{\mathbf{b}} + \chi_{iso}\underline{\mathbf{I}}\right]\cdot\nabla T\,;\qquad \chi_\| = 0.075, \quad \chi_{iso} = 7.5\times 10^{-6}$
  - $\underline{\Pi} = \nu_\| mn\left(\underline{\mathbf{I}} - 3\hat{\mathbf{b}}\hat{\mathbf{b}}\right)\hat{\mathbf{b}}\cdot\underline{\mathbf{W}}\cdot\hat{\mathbf{b}} - \nu_{iso} mn\underline{\mathbf{W}}\,;\quad \nu_\| = 5\times 10^{-2}, \quad \nu_{iso} = 5\times 10^{-5}$

    $\underline{\mathbf{W}} = \nabla\mathbf{V} + \nabla\mathbf{V}^T - \frac{2}{3}\underline{\mathbf{I}}\nabla\cdot\mathbf{V}$
- Artificial particle diffusivities are intended to be small.
  - $D_n = 5\times 10^{-6}, \quad D_h = 1\times 10^{-10}$
- NOTE: the equations used in this application have been normalized.
  - $\tau_A \equiv R_0^2 / F_{open} \cong 1; \quad \mu_0 \to 1, \quad n_0 \to 1$
  - $a \cong 1; \quad R_0 = 1.6$

We separate the problem into two coupled subdomains.

- Plasma responses are modeled in the central subdomain.
- The outer subdomain produces the vacuum magnetic response outside the resistive wall.
- Resistive diffusion through the wall is at an intermediate time-scale between τ_A and τ_η.
  - $v_{wall} = \eta_{wall} / \mu_0 \Delta x_{wall} = 1 \times 10^{-3}$
  - $\tau_A << \tau_w << \tau_\eta$
- Subdomains are coupled by the thin-wall model.

$$\frac{\partial \mathbf{B} \cdot \hat{\mathbf{n}}}{\partial t} = -\hat{\mathbf{n}} \cdot \nabla \times \left[v_w \hat{\mathbf{n}} \times \Delta \mathbf{B} \right]$$

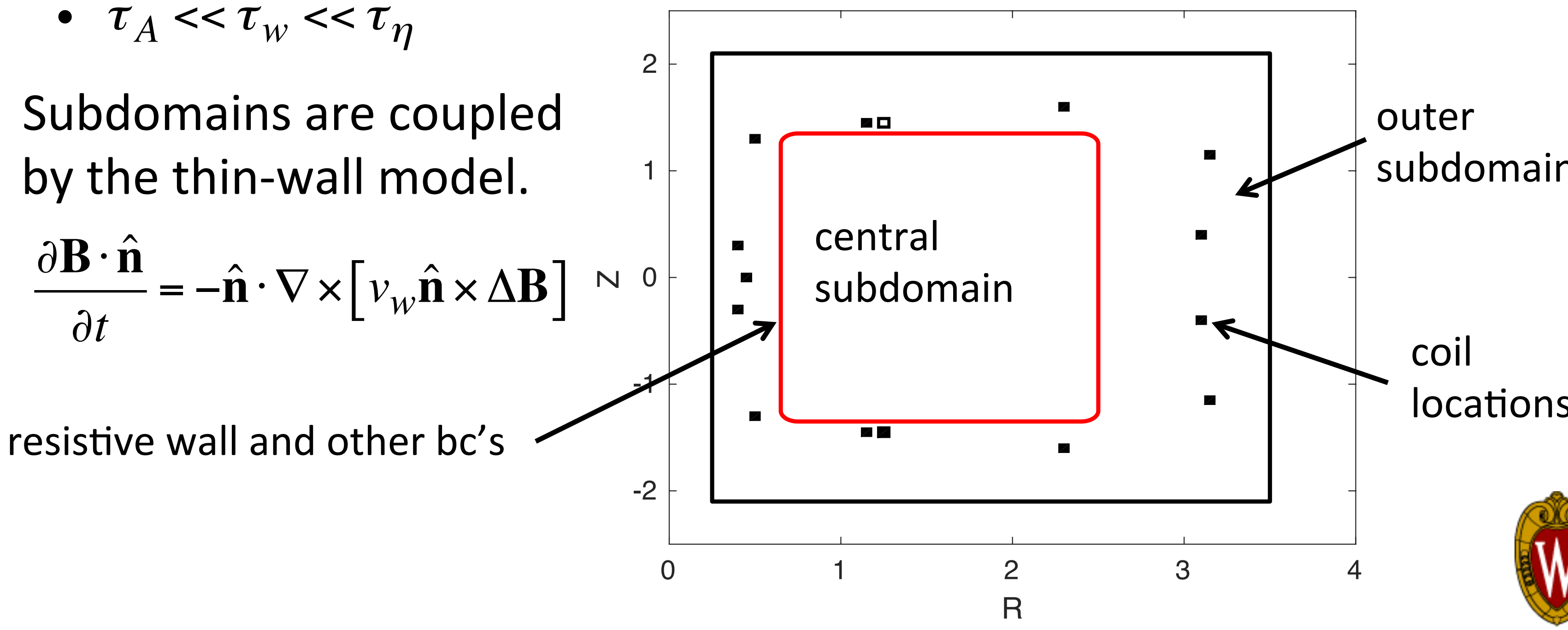

The computations start from an up-down symmetric equilibrium.

- $\beta(0) \cong 1\%$
- $q(0) = 1.75$

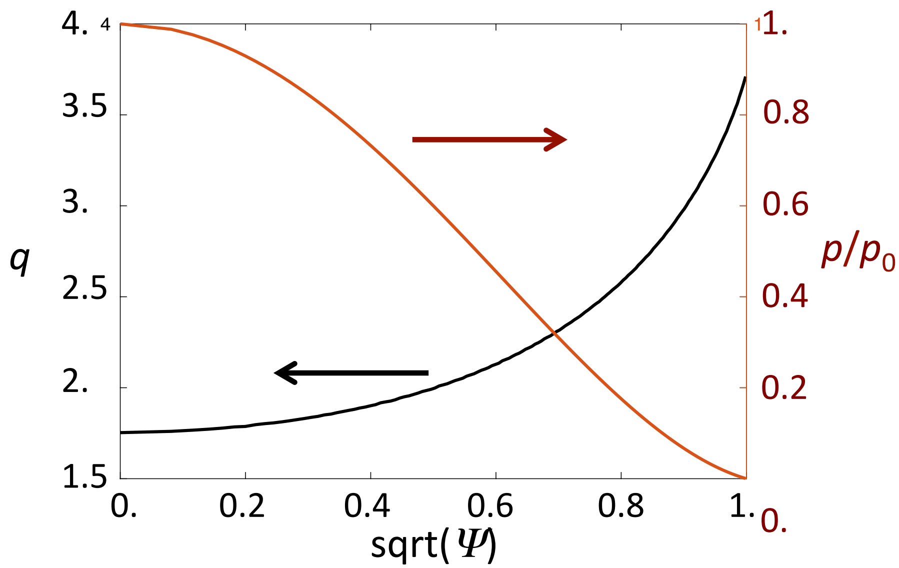

Safety factor and pressure profiles.

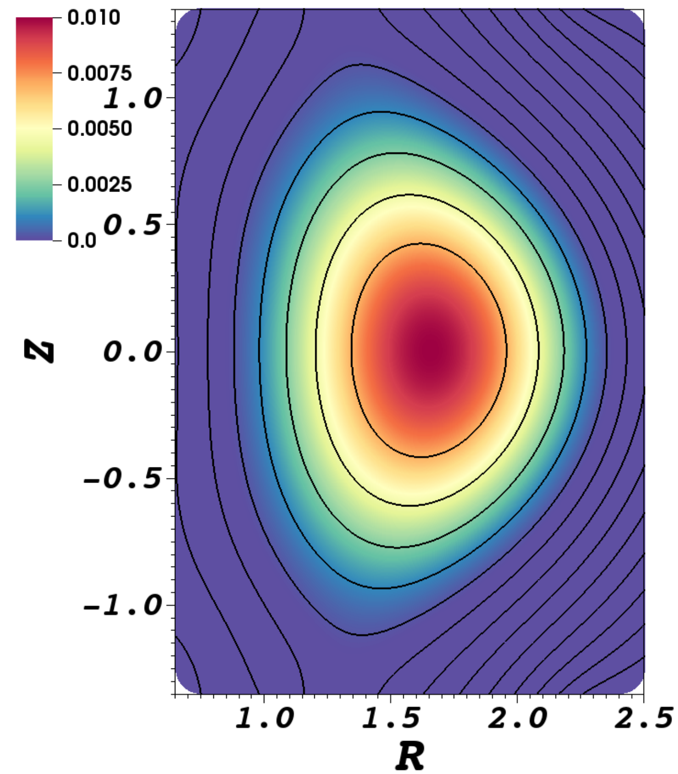

Contours of poloidal flux and pressure for the initial state. Border is the resistive wall.

- Forced VDEs are modeled by removing current from the upper divertor coil (outside the resistive wall).

Results of two nonlinear 3D computations are compared.

1. One models the effect of turning the upper divertor-coil off.
    - Plasma density and temperature, **B** from plasma current, and **B** from the upper divertor coil become part of the initial conditions.
    - Rest of external coil fields is held fixed.
    - Toroidal resolution evolves Fourier harmonics $0 \le n \le 21$.
    - The n = 1 and n = 2 harmonics have small fixed field errors; others have initial perturbations.
2. The second case holds all coil fields fixed, so there is no vertical forcing.

General Evolution: Distinct behavior results in each 3D computation and in a 2D case.

- The 3D computation with forcing produces a thermal quench (TQ) that is faster than the current quench (CQ).
- The forced 3D computation has the largest current bump.

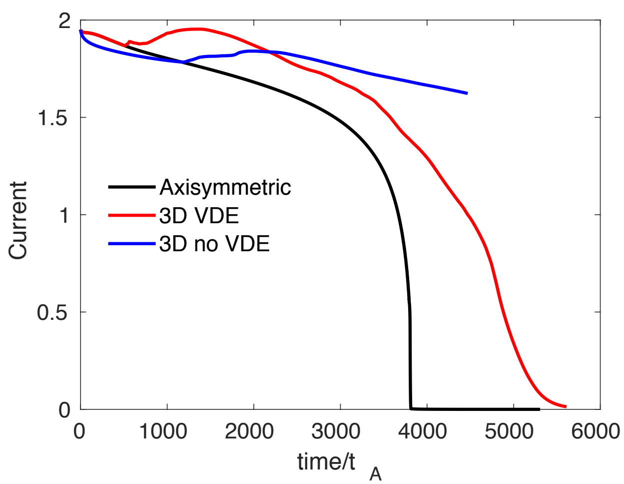

Plasma Current

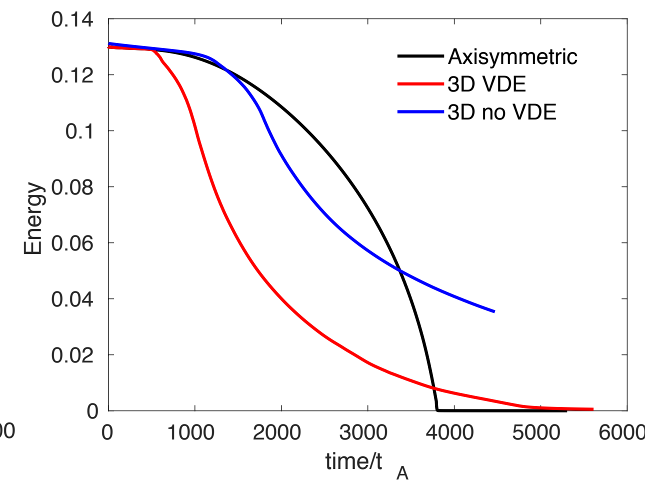

Thermal Energy

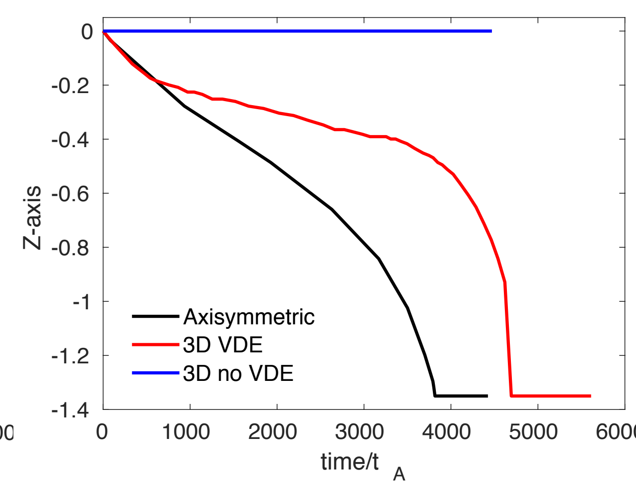

Vertical Position of Magnetic Axis

- The 3D computation without forcing exhibits a minor disruption without a CQ.

MHD activity develops and evolves throughout the 3D computation with forced displacement.

- The computed MHD activity does not display a simple saturation process.

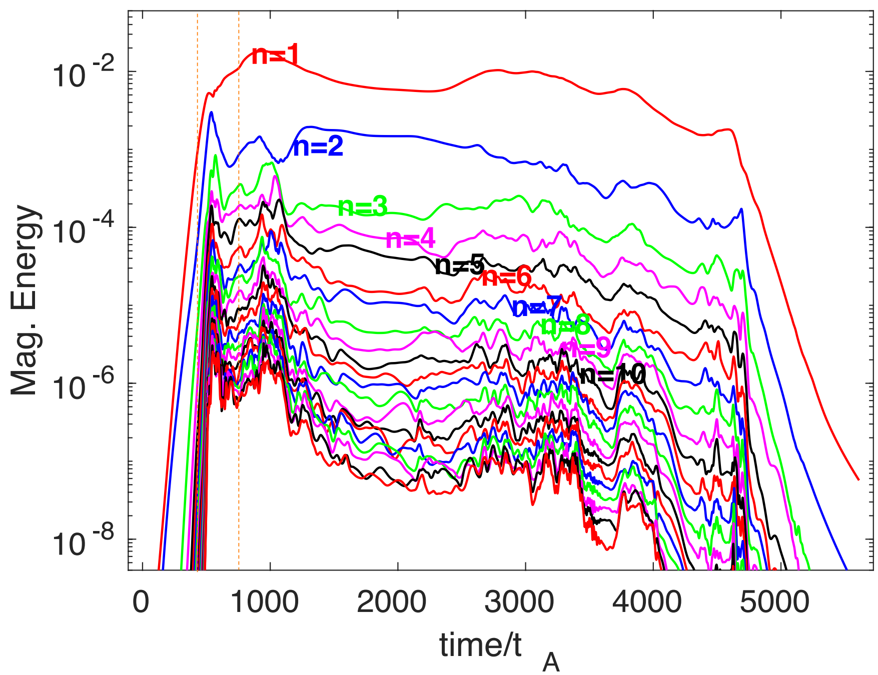

Magnetic energy fluctuations (1≤*n*≤21) are dominated by *n* = 1. Vertical lines show *t*=473 and *t*=759.

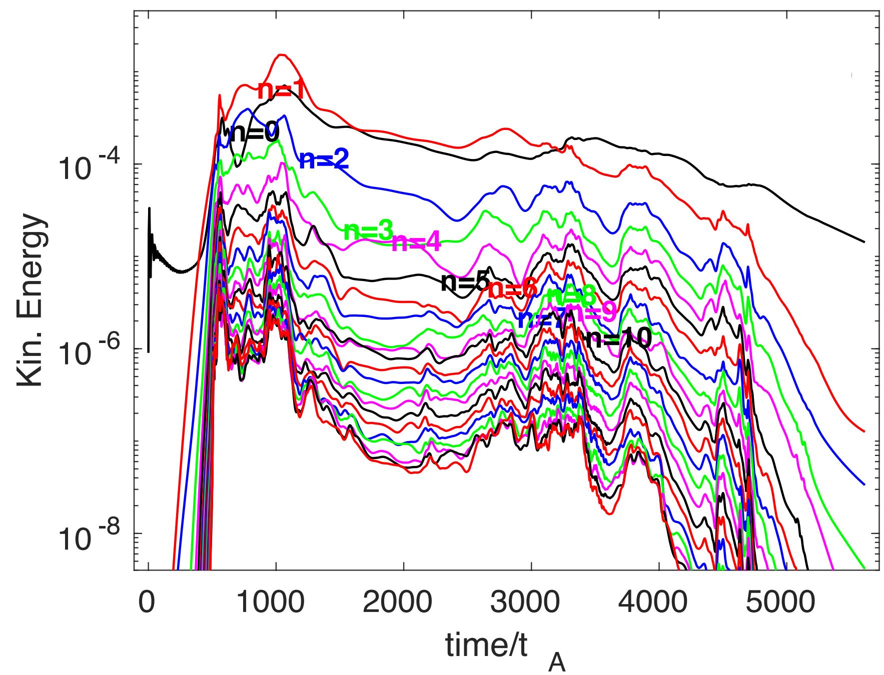

Kinetic energy spectrum is plotted with *n* = 0.

The dominant mode changes quickly with wall contact in the 3D case with forced displacement.

- Plots at right are at the times indicated on the previous slide.
- Resistive dissipation of the edge suppresses an initial *m* = 4 linear instability and excites *m* = 3.
- Contact with the wall accelerates a transition to *m* = 2.

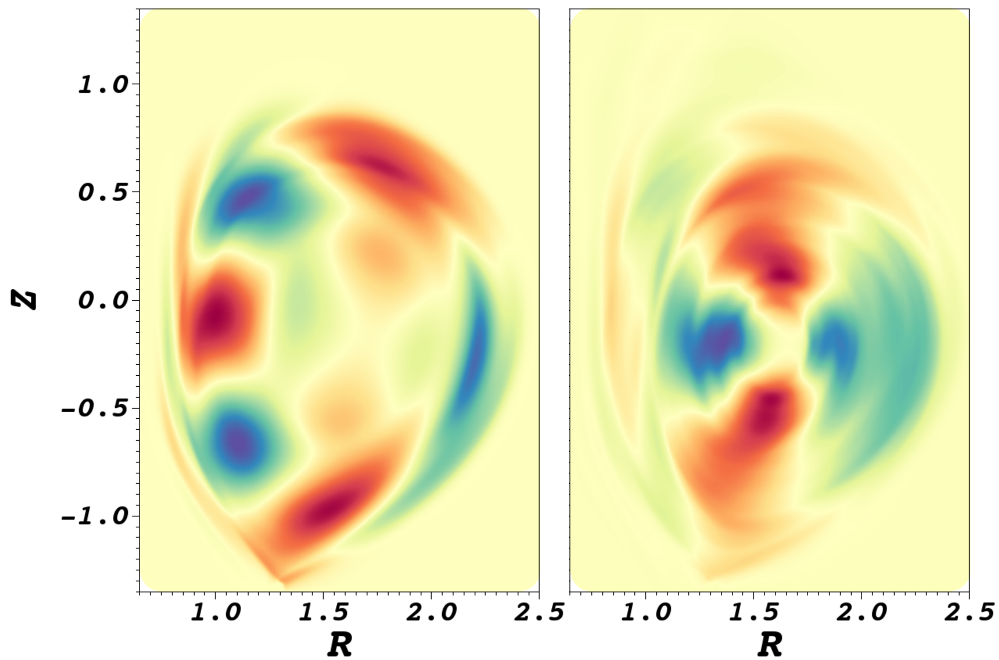

At *t* = 473, *n* = 1 pressure contours primarily show *m* = 3.

At *t* = 759, *n* = 1 perturbations are primarily *m* = 2.

As the dominant mode changes from *m* = 3 to *m* = 2, loss of flux surfaces initiates the thermal quench.

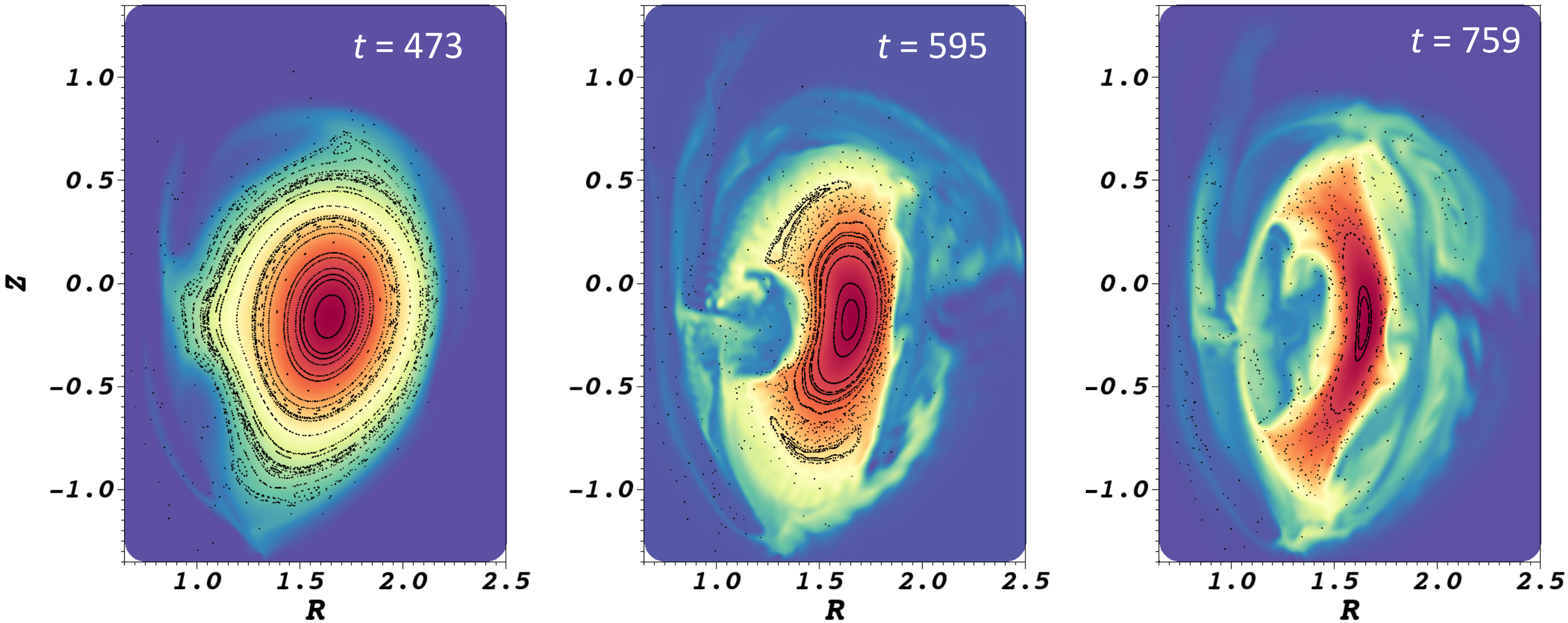

- Poincaré surfaces of section overlaid on pressure show the topology changes that lead to energy loss.
- Flux surfaces are not recovered in this case with forced displacement.

In the 3D computation without forcing, the initial growth is slower and takes longer to saturate.

- Resistive dissipation of the edge again excites MHD activity.
- This process is muted without the vertical displacement into the wall.

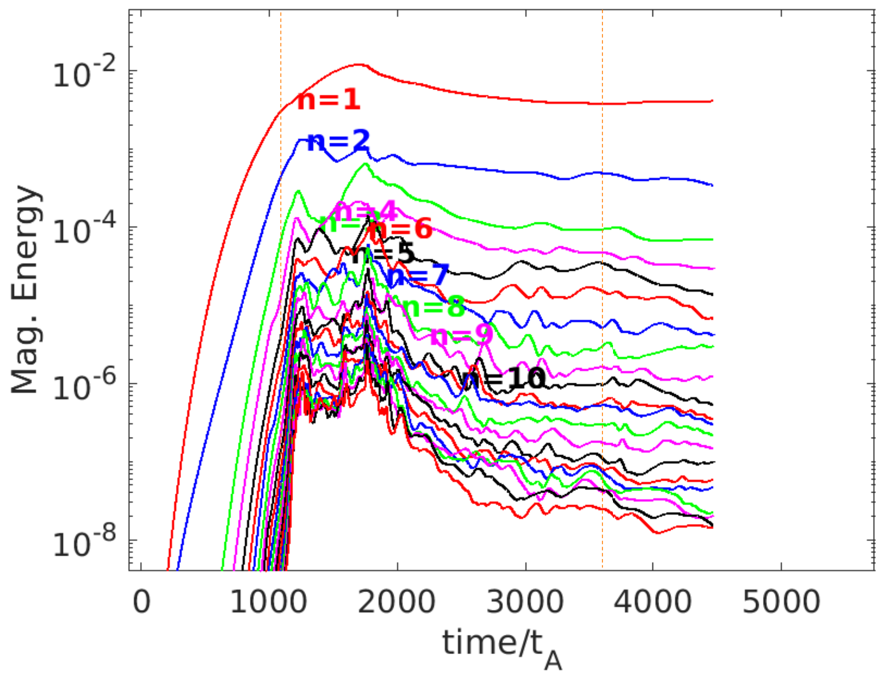

Magnetic energy fluctuations (1≤*n*≤21) are again dominated by *n* = 1. Vertical lines indicate *t*=1062 and *t*=3600.

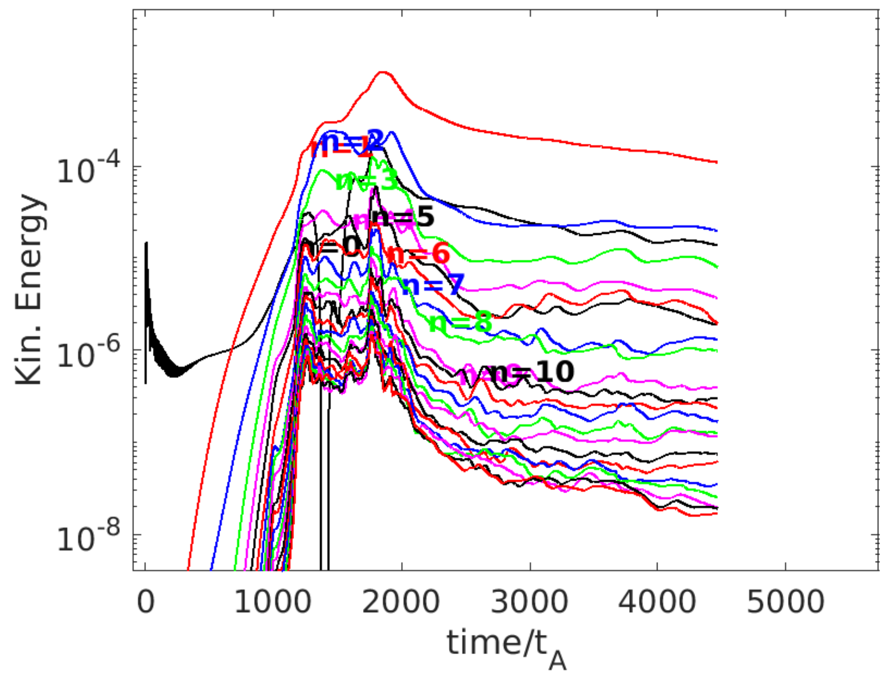

Kinetic energy fluctuations decay after the initial saturation.

The transition from $m = 3$ to $m = 2$ also occurs without vertical forcing, but the result is just a minor disruption.

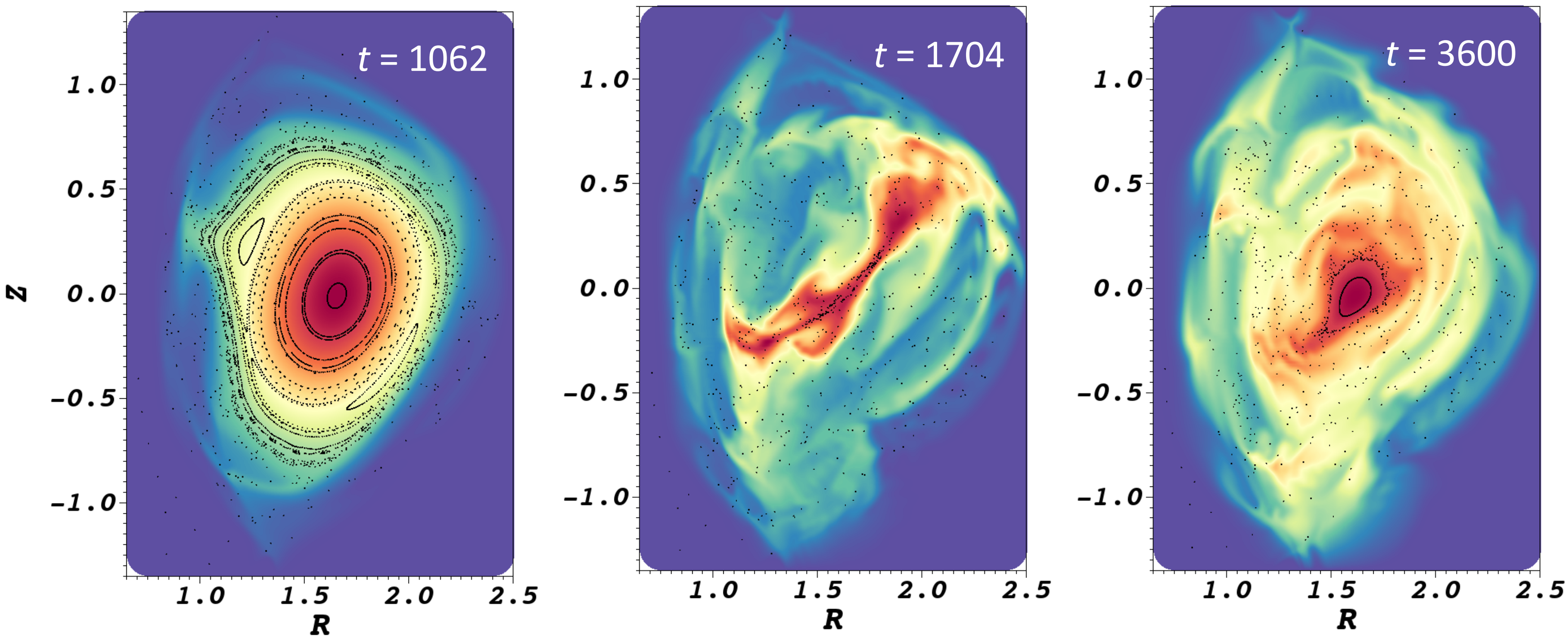

- Maximum pressure remains at 94% of its initial value through t=1700; by t=3600 it has decreased to 27%.
- Central closed flux surfaces are recovered after thermal energy is lost.
- There is no CQ through the end of the computation.

Current Spike: 3D spreading of current density that increases I_p can be described as a dynamo effect.

- The parallel current density $\langle J_{||}\rangle/\langle B\rangle$ and poloidal flux distributions broaden when I_p increases.

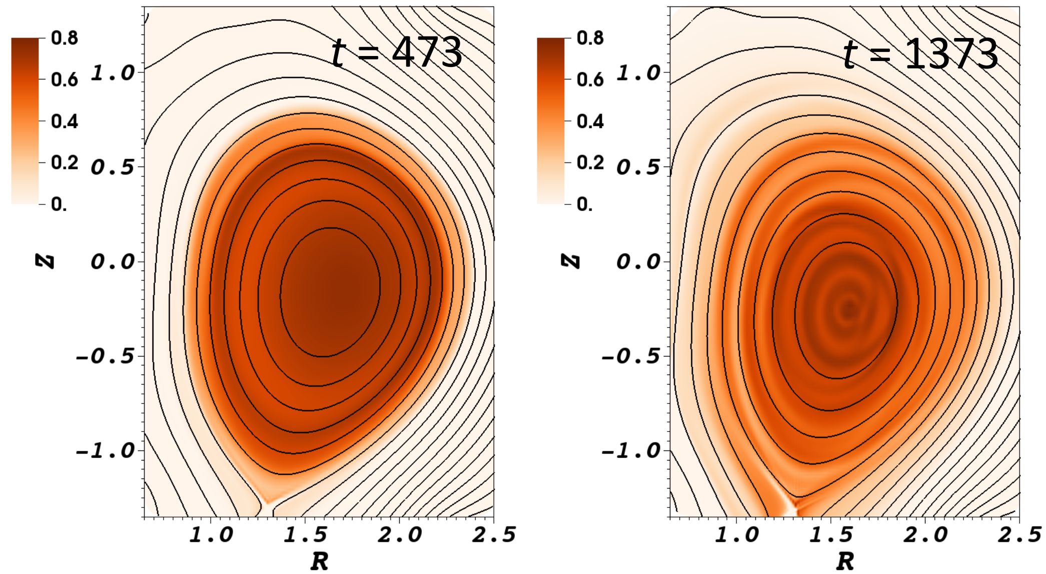

- Correlated fluctuations of flow velocity and magnetic field induce changes in spatially averaged **B**.
  - Averaged Faraday's law with resistive-MHD **E**:

$$\frac{\partial}{\partial t}\langle \mathbf{B}\rangle = -\nabla\times\left[\langle \eta \mathbf{J}\rangle - \langle \mathbf{V}\rangle\times\langle \mathbf{B}\rangle + \mathbf{E}_f\right]$$

  - MHD dynamo effect from astrophysics, RFP, and spheromak literature is $\mathbf{E}_f = -\langle \tilde{\mathbf{v}}\times\tilde{\mathbf{b}}\rangle$ [e.g., Moffat (1978) and Schnack, et al. Phys. Fluids **28**, 321].

dI_p/dt becomes positive when power transferred by $\mathbf{E}_f$ is large.

- Low-frequency Poynting theorem for $\langle \mathbf{B} \rangle^2$ evolution is
$$\frac{\partial}{\partial t}\frac{\langle \mathbf{B} \rangle^2}{2\mu_0} + \frac{1}{\mu_0}\nabla \cdot \langle \mathbf{E} \rangle \times \langle \mathbf{B} \rangle = -\langle \mathbf{E} \rangle \cdot \langle \mathbf{J} \rangle$$
- Right side includes fluctuation-induced $-\mathbf{E}_f \cdot \langle \mathbf{J} \rangle$.
- In the core, maximum $\left| \mathbf{E}_f \right|$ exceeds $\langle \eta \rangle \langle J_\phi \rangle$ by more than 10.

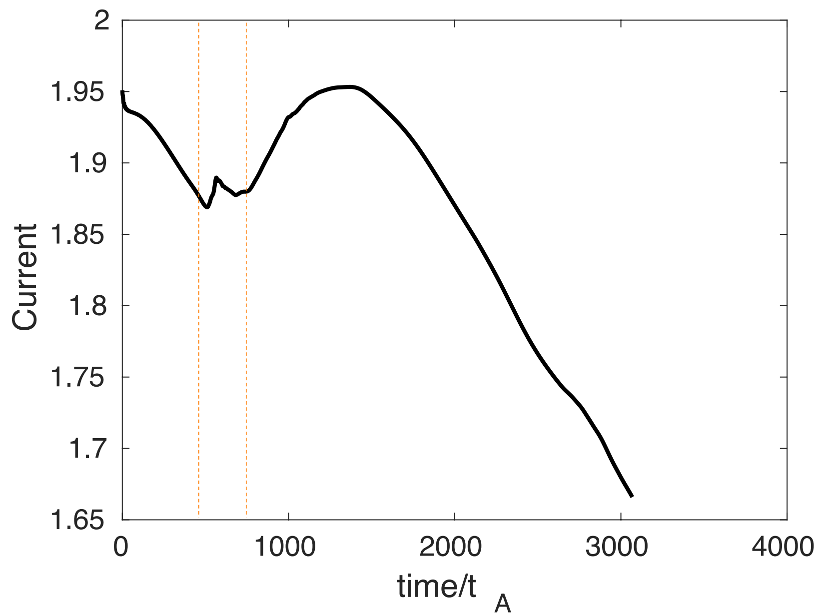

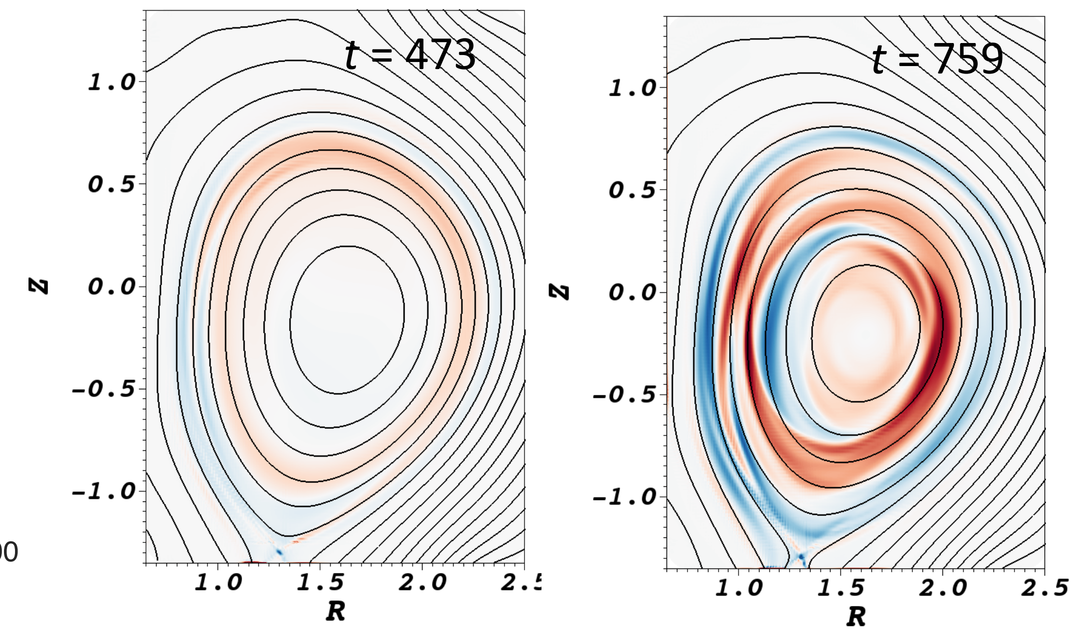

Plasma current bump occurs when *m*=2 becomes dominant.

Blue contours show $\langle E_f \rangle . \langle J \rangle < 0$, red is >0, overlaid with poloidal flux contours.

"Relaxation" of parallel current density is not as uniform as it appears in plots of averaged field.

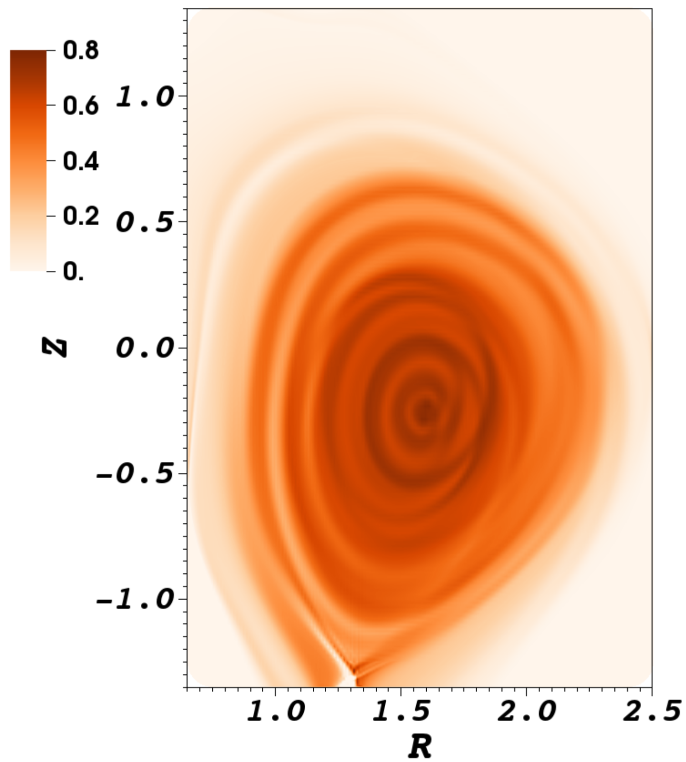

Plot of $\langle \mu_0 J_{||}/B \rangle$ at t = 1373 τ_A of the new simulation, where < > indicates toroidal average.

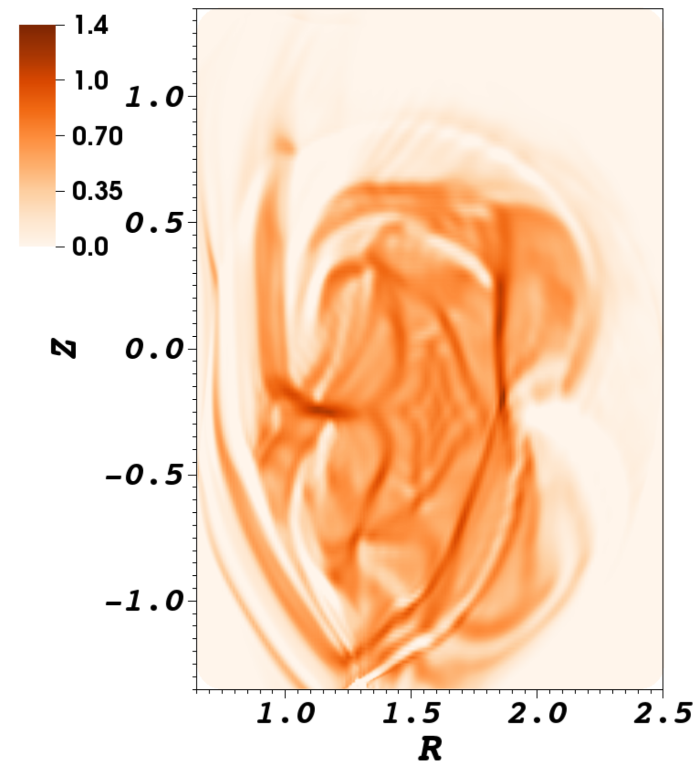

Plot of $\mu_0 J_{||}/B$ over one poloidal slice at t = 1373 τ_A.

Wall Forces: Forces with a thin-wall model can be computed from integrating stress over the outer surface.

- Pustovitov's computation [Nucl. Fusion **55**, 113032] is the natural one to apply with thin-wall modeling.
  - It assumes that the wall and plasma form an electrically isolated system.
  - Plasma inertial force is negligible on τ_{wall} timescale.
- Cartesian components of Lorentz force over any object are $F_j = \hat{\mathbf{e}}_j \cdot \int \mathbf{J}\times\mathbf{B}\, dVol$.
  - With a thin wall, $\mathbf{J}\Delta x \rightarrow \mathbf{K}$ as $|\mathbf{J}| \rightarrow \infty$, but

    $F_j = \mu_0^{-1} \oint d\mathbf{S}\cdot\left[\mathbf{BB} - \underline{\underline{\mathbf{I}}}\, B^2/2\right]\cdot\hat{\mathbf{e}}_j$ holds.
  - Split into integrals over inner and outer surfaces of the wall:

    $$F_{in_j} = \mu_0^{-1} \int_{S_{in}} d\mathbf{S}\cdot\left[\mathbf{BB} - \underline{\underline{\mathbf{I}}}\, B^2/2\right]\cdot\hat{\mathbf{e}}_j\,; \quad F_{out_j} = \mu_0^{-1} \int_{S_{out}} d\mathbf{S}\cdot\left[\mathbf{BB} - \underline{\underline{\mathbf{I}}}\, B^2/2\right]\cdot\hat{\mathbf{e}}_j$$
  - Also, $-F_{in}$ acts on plasma, hence $F_{in} \rightarrow 0$ for negligible plasma inertia.

    $F_j \rightarrow F_{out_j}$

Our computations are consistent with Pustovitov's analysis.

- We compute both F_{out} and F_{in} for the 3D computation with forcing.
- Computed results have $F_{in_j} \sim \frac{1}{100} F_{out_j}$.

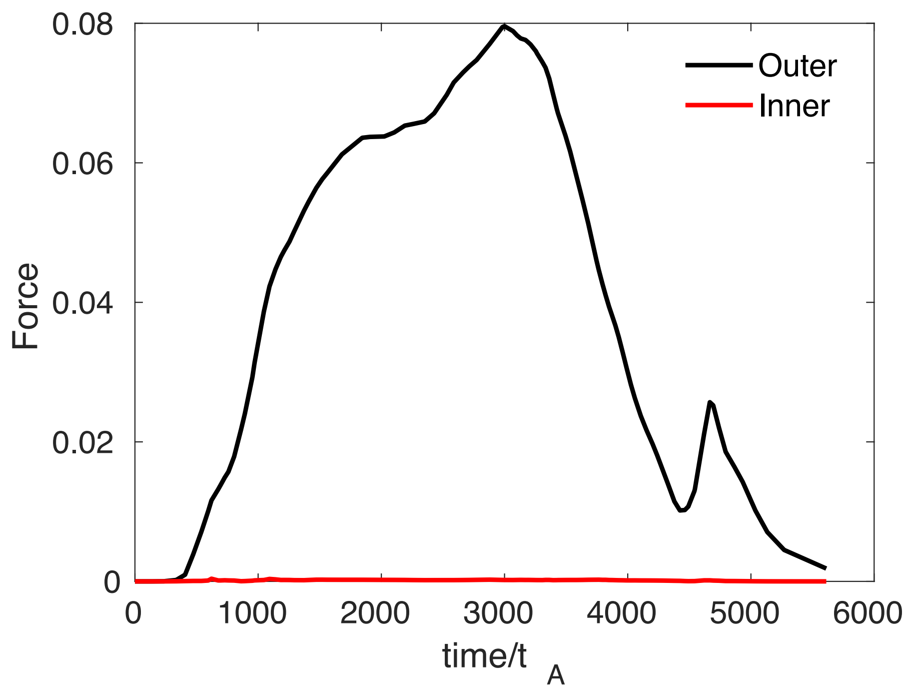

Integrated horizontal forces F_{out} and F_{in}.

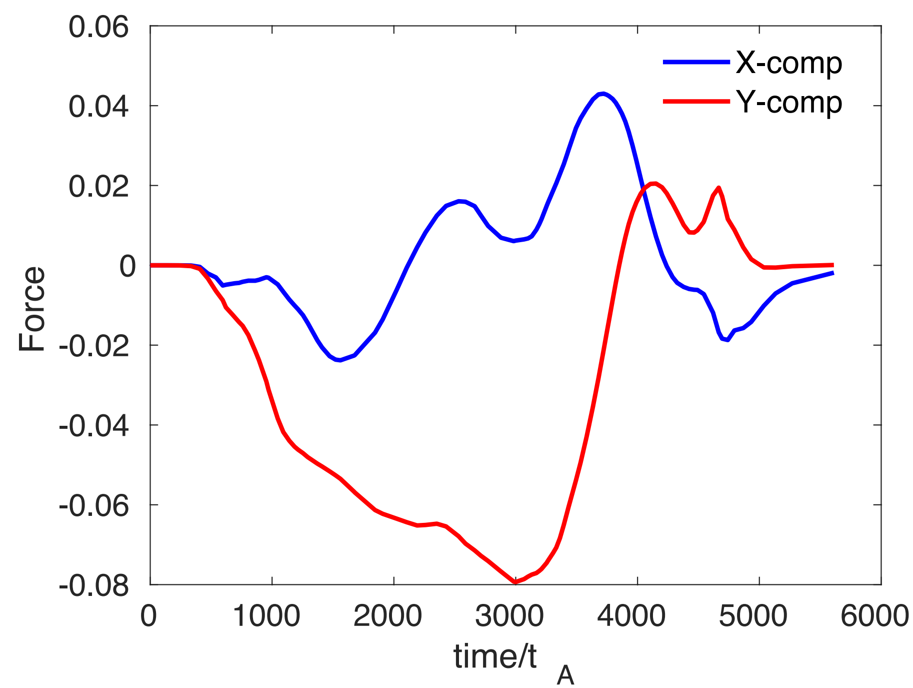

Horizontal force broken into components.

Local forcing may exceed expectations from the magnitude of net forces.

- Force per unit area is $\frac{1}{\mu_0}\hat{\mathbf{n}}\cdot\Delta\left(\mathbf{BB}-\underline{\mathbf{I}}\frac{B^2}{2}\right)$, where Δ means the jump over the surface.

- Spatially local forcing may cancel when integrated over the surface.

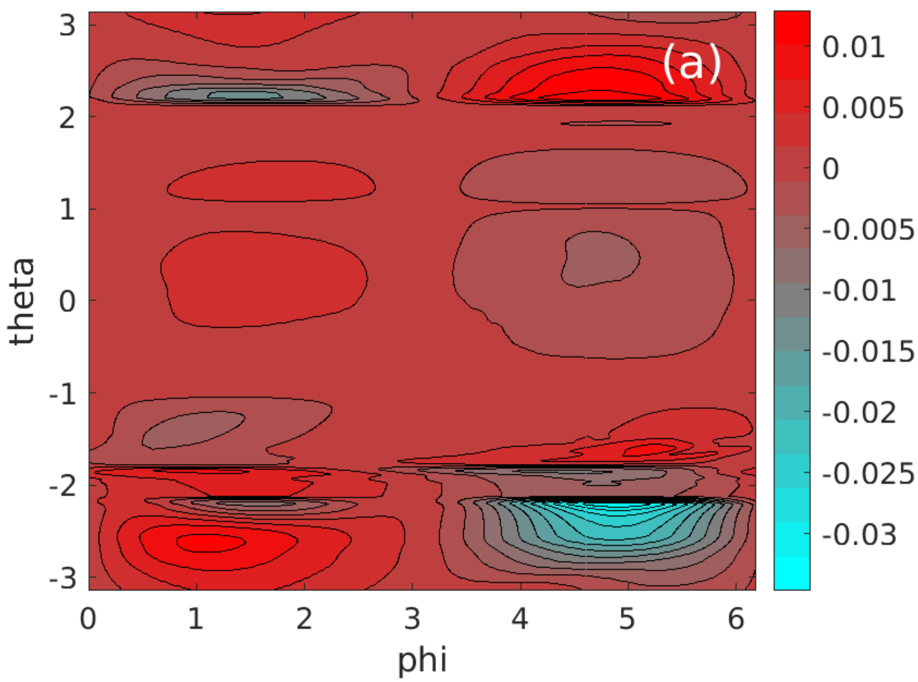

Cartesian *y*-component of force per unit area at *t*=971 of the forced 3D computation.

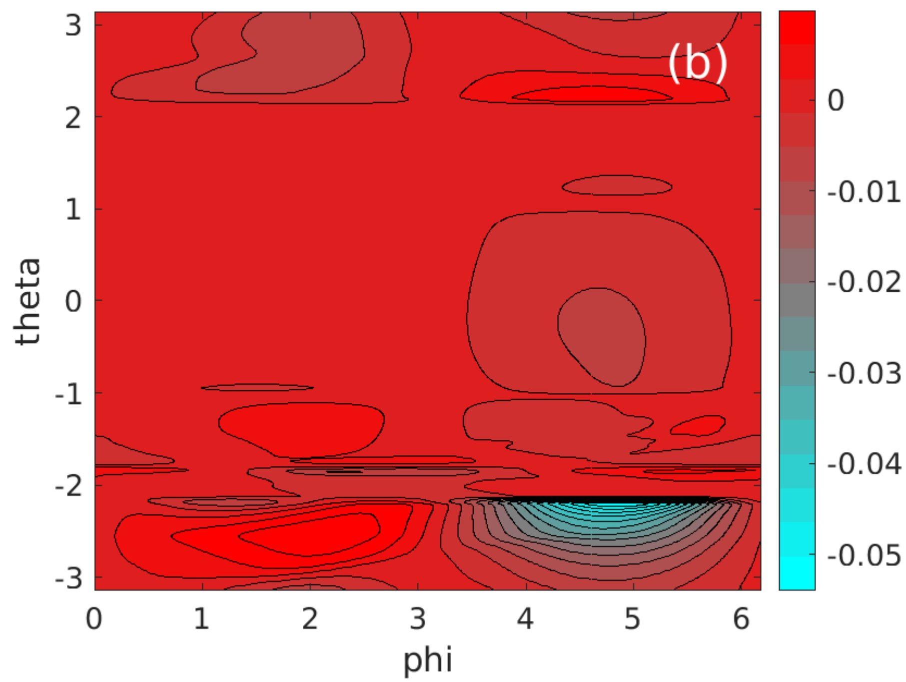

Force per unit area at *t*=3000, when net force peaks in the same computation.

Conclusions

- Visco-resistive MHD-based computations with NIMROD reproduce important qualitative features:
  - Relatively fast thermal quench
  - Current bump then relatively slow decay (even in the absence of a RE modeling)
- Current bump occurs after TQ has begun, and dynamo effect is relevant.
- Wall-force check supports Pustovitov's approach to computing net force.
- Stresses that contribute to net force may be concentrated.
  - Local forcing may cause more damage than net force.